

ULRR

Preparation of new doxycycline monohydrate polymorphs by ultrasonication enhanced supercritical antisolvent recrystallization process

| | |
|---------------|---|
| Item Type | Article |
| Authors | Nandi, Snehashis;Rodrigues, Miguel A.;Duarte, Andreia;Nunes, Teresa G. |
| Citation | Journal of CO2 Utilization 96, 103082 |
| Publisher | Elsevier |
| Download date | 2026-03-05 11:59:54 |
| Item License | https://creativecommons.org/licenses/by-nc-sa/4.0/ |
| Link to Item | https://doi.org/10.34961/researchrepository-ul.29194760 |



Preparation of new doxycycline monohydrate polymorphs by ultrasonication enhanced supercritical antisolvent recrystallization process

Snehashis Nandi^{a,b}, Miguel A. Rodrigues^c, Andreia Duarte^c, Teresa G. Nunes^c, Luis Padrela^{a,b,*}

^a Department of Chemical Sciences, Bernal Institute, University of Limerick, Limerick V94 T9PX, Ireland

^b SSPC, The Research Ireland Centre for Pharmaceuticals, Bernal Institute, University of Limerick, V94 T9PX, Ireland

^c Centro de Química Estrutural and Department of Chemical Engineering, Instituto Superior Técnico, Universidade de Lisboa, Av. Rovisco Pais, Lisboa 1049-001, Portugal

ARTICLE INFO

Keywords:

Doxycycline monohydrate
Ultrasonication
UE-SAR
DoE
Polymorphism
Thermal stability

ABSTRACT

Polymorphism is a crucial factor in the pharmaceutical industry, as different polymorphs can display different physicochemical properties, including stability, solubility, and/or bioavailability. The ultrasonication-enhanced supercritical antisolvent recrystallization (UE-SAR) process is a novel investigated approach for producing novel polymorphs. This work aimed to generate and characterize doxycycline monohydrate (DOXY·H₂O forms II, III, and IV) polymorphs produced from suspensions of its as received form (DOXY·H₂O form I) using the UE-SAR process. A two-stage Design of Experiments (DoE) analysis was performed to assess the impact of various processing parameters such as ultrasonication, pressure, temperature, and residence time on the polymorphic outcome in each experimental run. The solid state characterization revealed that the produced polymorphs (DOXY·H₂O form II, DOXY·H₂O form III) have distinct powder X-ray diffraction (PXRD), Raman, Fourier Transform Infrared (FTIR) patterns and higher thermal stability. Moreover, the structures of DOXY·H₂O forms I and II were further elucidated by solid state nuclear magnetic resonance (SS NMR) from 13 C and 15 N cross polarization (CP) and magic angle spinning (MAS) spectra. Overall, the results from this work highlight that use US-SAR method can induce the formation of different supramolecular structures in tetracyclines when they are suspended in a supercritical phase, and polymorphic purity can be enhanced by prolonged ultrasonication.

1. Introduction

Polymorphs have the same chemical composition but different crystal structures, due to the ability of molecules to assemble into different crystal packing arrangements and/or conformations [1,2]. For the pharmaceutical industry, one of the main concerns nowadays is whether an active pharmaceutical ingredient (API) can crystallize or interconvert into different polymorphic forms during processing or shelf life, as different polymorphs can display different physicochemical properties including stability, solubility, and/or bioavailability [3]. Pharmaceutical crystallization processes require ever-greater understanding and control since polymorphism is one of the primary controlling factors that directly affects a drug substance's processability as well as the quality, safety, and efficacy of a drug product [4]. Due to their slow nucleation and crystal growth kinetics, conventional crystallization methods such as cooling crystallization and solvent evaporation take a very long time to form crystals. Antisolvent crystallization

techniques offer much faster nucleation and crystal growth kinetics, usually favoring the formation of metastable polymorphic forms and smaller crystals. These techniques involve adding a nonsolvent (typically water) to a saturated solution in order to induce the precipitation of the solute. Further filtration and drying procedures are necessary when using liquid antisolvent crystallization techniques to remove any remaining organic solvent from the final particles [5]. The use of supercritical CO₂ instead of water eliminates the possibility of formation of hydrates, and the final product is left solvent-free after the crystallization process when the residual organic solvent is flushed with CO₂ [6]. Over the last decade, particle engineering and solid-state chemistry with supercritical fluids have been widely described in pharmaceuticals [7,8]. Moreover, supercritical CO₂ (scCO₂) has been used in the development of new crystalline forms of APIs, due to its miscibility with organic solvents, which promotes and enables the assembly of novel crystalline structures [9–11]. Since solvent removal and recovery in supercritical antisolvent recrystallization (SAR) are easier compared to liquid

* Corresponding author at: Department of Chemical Sciences, Bernal Institute, University of Limerick, Limerick V94 T9PX, Ireland.

E-mail address: Luis.Padrela@ul.ie (L. Padrela).

<https://doi.org/10.1016/j.jcou.2025.103082>

Received 15 November 2024; Received in revised form 10 April 2025; Accepted 10 April 2025

Available online 30 April 2025

2212-9820/© 2025 The Author(s). Published by Elsevier Ltd. This is an open access article under the CC BY license (<http://creativecommons.org/licenses/by/4.0/>).

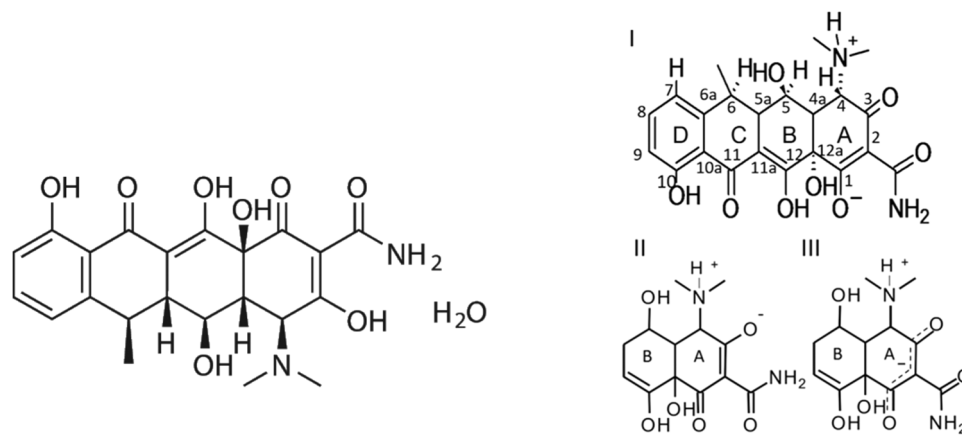


Fig. 1. Chemical structure of (Left) Doxycycline monohydrate (DOXY·H₂O form I), along with (Right) tautomer I [19] and rings A and B in another zwitterionic tautomers: II (“enol”) and III (“keto”).

antisolvent processes, SAR is environmentally more acceptable. Consequently, in order to make pharmaceutical products on an industrial scale, a wash-out procedure by SAR might be required [12]. Although extensive research has been carried out on SAR methods [10,13,14], to the best of our knowledge no single study in the literature has addressed the recrystallization of a novel polymorphic form of an API from a suspension (as clear liquid solutions containing the API dissolved are typically used in SAR methods), discarding the requirement of the API solubility in the selected liquid solvent.

Doxycycline (α -6-deoxyoxytetracycline, DOXY) has been used as a model system in this work. It is a broad-spectrum antibiotic of the tetracyclines class, and within its class, is the most used drug due to the efficacy, low side effects and low cost [15,16]. DOXY is available in three forms: monohydrate (4 - (dimethylamino) - 1,4,4a,5,5a,6,11,12a - octahydro - 3,5,10,12,12a - pentahydroxy - 6 - methyl - 1,11 - dioxo - 2 - naphthacene-carboxamide monohydrate) (DOXY·H₂O form I), hydrochloride dihydrate (DOXY·HCl·2H₂O) and hyclate (DOXY·HYC, DOXY·HCl·(H₂O)_{0.5}·(C₂H₅OH)_{0.5}), a hemithanolate-hemihydrate hydrochloride which is a broad-spectrum antibiotic used worldwide to treat infectious diseases. In this work, a novel polymorphic form of doxycycline monohydrate (DOXY·H₂O form II) is reported after being recrystallized from suspensions of its as-received form (DOXY·H₂O form I) in scCO₂ with a co-solvent (e.g., ethanol) by the SAR method. This technique was successfully used previously to recrystallize a different antibiotic (e.g., minocycline hydrochloride) into a new anhydrous form [17], suggesting that scCO₂ could be used to remove hydration water from antibiotic crystals. The objective of this work is thus to propose a Design of Experiments (DoE) approach for screening the pertinent factors that influence the performance of the SAR process. Furthermore, this study also reports and investigates a novel ultrasonication enhanced supercritical antisolvent recrystallization (UE-SAR) developed in this work, assessing the influence of its operational parameters (e.g., pressure, temperature, and residence time of crystallization) on the novel polymorph formation using a central composite DoE. The process response is only focused on the polymorphic outcome of the generated DOXY·H₂O crystals. The generated DOXY·H₂O crystals were analyzed to compare the effects of SAR and UE-SAR processes on the polymorphic purity by using powder X-ray diffraction (PXRD). Thereafter, the novel forms of DOXY·H₂O were characterized in-detail by PXRD, differential scanning calorimetry (DSC), fourier transform infrared (FTIR) and Raman spectroscopy, scanning electron microscopy (SEM), Karl Fischer titration and thermal analysis. Specifically, solid-state nuclear magnetic resonance (SS NMR) spectroscopy was used to elucidate the crystal structures of forms I and II, which is provided in the [Supplementary Information](#).

Table 1

Information on the physicochemical properties of Doxycycline monohydrate (DOXY·H₂O form I) used in this study [18].

| Properties | Value |
|------------------|---|
| Chemical class | Tetracycline antibiotic |
| Molecular weight | 462.4 g/mol |
| log P | -0.72 |
| Chemical formula | C ₂₂ H ₂₆ N ₂ O ₉ |
| Melting point | 163 °C |
| Stability | -20 °C, 12 h at 25 °C, 6 h in solution |

2. Experimental section

2.1. Materials and methods

Fig. 1. Doxycycline monohydrate (DOXY·H₂O form I) was sourced from Sigma Aldrich (Belgium). Absolute ethanol (99.5 %) was supplied by BASF (Germany). Carbon dioxide (99.98 %) pure was supplied by BOC (Ireland). Physicochemical properties of DOXY·H₂O form I are described in [Table 1](#).

2.2. Supercritical antisolvent recrystallization (SAR)

The SAR apparatus represented in more detail in [Fig. 2](#) comprises a 10 cm³ stainless steel high-pressure reaction vessel (where recrystallization occurs) with a borosilicate glass window (Maxos™, Auer Lighting, Germany), with an inlet and outlet ports. Pressure and temperature were measured using, respectively, a pressure transducer (Omega model PX603) and a T-type thermocouple assembly (Omega). These vessels were placed inside a temperature-controlled air chamber by using a controller from Ero Electronic (model LDS) and a T-type thermocouple (Omega) to maintain the scCO₂ properties and ongoing reaction at the set temperature. A borosilicate glass window fitted on the top of the high-pressure vessel was used for visualization purposes during the experiments.

Doxycycline monohydrate (DOXY·H₂O form I) and ethanol mixtures in a mass proportion of 1:10 (200 mg of DOXY·H₂O to 2 g of ethanol) were loaded in the recrystallization chamber schematically shown in [Fig. 3](#). This DOXY·H₂O suspension was mixed with CO₂ until the working pressure reached the desired value according to the DoE points (1–9) and for 9 R, changing in a mass proportion of 1:50 (100 mg of DOXY·H₂O to 5 g of ethanol) keeping other parameters constants, represented by [Table 2](#). The mixture was stirred at 400 rpm using a magnetic stirrer (Selecta, model Agimatic-N) during the experiments. The procedure was continued for three different residence time intervals. Afterwards, the recrystallization cell was flushed to remove the ethanol

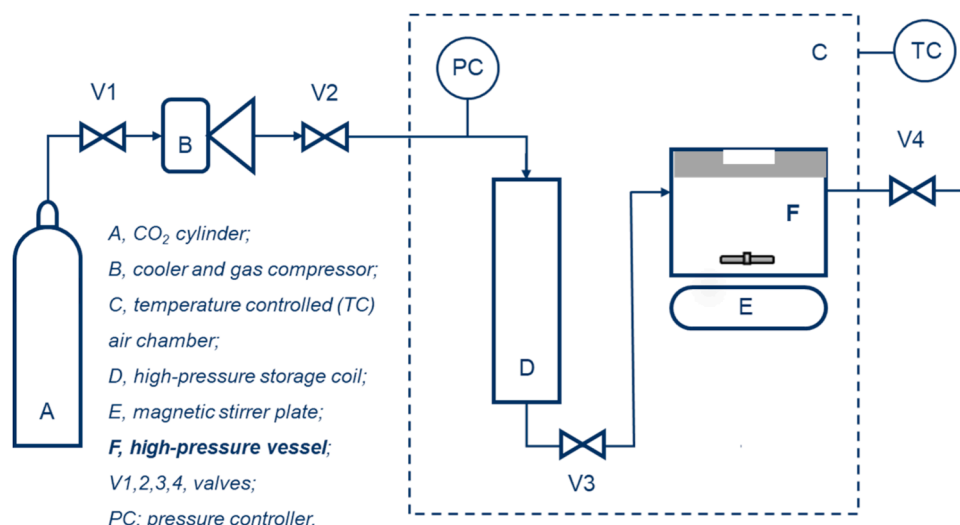


Fig. 2. Schematic diagram of experimental setup for the supercritical antisolvent recrystallization process.

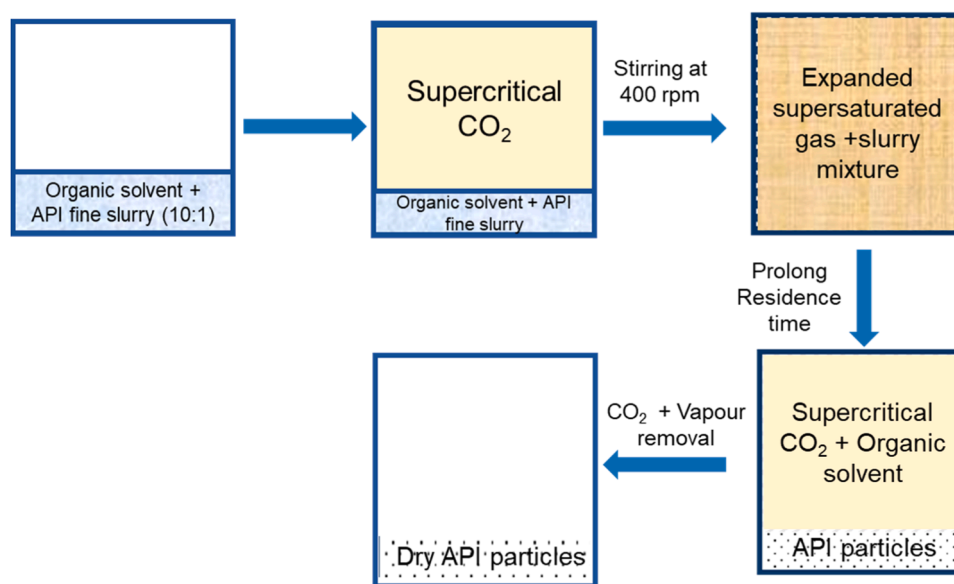


Fig. 3. Process flow diagram of supercritical antisolvent recrystallization (SAR) method for the generation of doxycycline monohydrate (DOXY·H₂O) polymorphs.

with a flow of 2 g/min of fresh CO₂ for 25 min duration. Finally, the recrystallization cell was slowly depressurized, and the resulting material was collected and stored in a closed desiccator before solid-state characterization.

2.3. Ultrasonication-enhanced supercritical antisolvent recrystallization (UE-SAR)

The UE-SAR process is further modified as presented in the schematic flow diagram in Fig. 4. DOXY·H₂O form I and ethanol mixture in a mass proportion of 1:50 (100 mg of DOXY·H₂O to 5 g of ethanol) was stirred on a magnetic stirrer for 10 min at 1200 rpm to form a homogenous suspension. The sample was then placed under an ultrasonic probe for 35 minutes at 25 °C at an amplitude of 80 %. The Syclon Ultrasonic Homogenizer (250 W, 20 kHz, 3 mm probe) was used to generate the ultrasound effect. The temperature was controlled using a water bath placed below the sample. After that, the fine suspension was loaded in the recrystallization chamber and was stirred at 1200 rpm during the entire process. Afterwards, the recrystallization cell was flushed to

remove the ethanol with a flow of 2 g/min of fresh CO₂ for 60 min duration. This step was repeated three times to ensure complete removal of ethanol from the solids. Finally, the recrystallization cell was slowly depressurized, and the resulting material was collected and stored in a closed desiccator before solid-state characterization. The samples were stored in a closed desiccator before solid-state characterization.

2.4. Design of experiments based study

A study using a three-factor two-level full factorial DoE with centre points was performed to investigate the influence of the SAR processing variables (pressure, temperature, and residence time) on the polymorph generation of doxycycline monohydrate crystals. The description of the DoE is presented in Table 2. The pressure varied between 90 and 200 bar while the temperature varied between 25 and 60 °C. The residence time for recrystallization varied between 1 and 8 hours. An identical set of DoE experiments was also performed using the UE-SAR process to investigate the impact of ultrasonication (as indicated in Table 2; Fig. 4). The stirring rate (at 400 rpm), API to ethanol mass ratio 1:10, and

Table 2

A central composite Design of experiment (DoE) study for operating conditions for the supercritical antisolvent recrystallization (SAR) (DoE points 1–9, 9 R), and ultrasonication-enhanced supercritical antisolvent recrystallization (UE-SAR) processes (DoE points 1–9), and for ultrasonication followed by slow evaporation (DoE point 10).

| DoEpoint | Pressure(bar) | Temp(°C) | Residence time (h) |
|----------|---------------|----------|--------------------|
| 1 | 90 | 25 | 1 |
| 2 | 90 | 60 | 1 |
| 3 | 200 | 60 | 1 |
| 4 | 200 | 25 | 1 |
| 5 | 90 | 25 | 8 |
| 6 | 90 | 60 | 8 |
| 7 | 200 | 60 | 8 |
| 8 | 200 | 25 | 8 |
| 9 | 150 | 40 | 4 |
| 9 R | 150 | 40 | 4 |
| 10 | 1 | 25 | - |

For the SAR process, constant parameters (agitation speed 400 rpm, API to ethanol mass ratio 1:10, number of CO₂ flushing cycles thrice for DoE points 1–9; agitation speed 1200 rpm, API to ethanol mass ratio 1:50, number of CO₂ flushing cycles thrice for DoE point 9 R). For the UE-SAR process, constant parameters (agitation speed 1200 rpm, API to ethanol mass ratio 1:50, CO₂ flushing cycles thrice for DoE points 1–9). DoE point 10 refers to the fine suspension sample, generated after the ultrasonication process, being kept under a slow evaporation process at 25°C and under atmospheric pressure.

number of CO₂ flushing cycle (once) were kept constant throughout the DoE experiments 1–9, whereas for DoE point 9 R (replicate of DoE 9), stirring rate increased to 1200 rpm, API to ethanol mass ratio increased to 1:50, and number of CO₂ flushing cycles increased to thrice. For the UE-SAR process, similar stirring rate, API to ethanol mass ratio and number of CO₂ flushing cycles were kept as mentioned in DoE point 9 R for the SAR process. All DoE experiments for both SAR and UE-SAR methods were performed in duplicates and DoE point 3 for UE-SAR process was repeated thrice. JMP Pro® 17.0 software was used to analyze the data.

An additional control study (mentioned as DoE point 10) was performed in duplicates where the fine suspension generated after the ultrasonication process was kept under a slow evaporation process at 25°C and air pressure to monitor the polymorphic form obtained over a longer period. Upon completion, the samples were analyzed for detailed solid-state characterization.

2.5. Solid state characterization

2.5.1. Powder X-ray diffraction (PXRD)

PXRD was used to identify the solid-state and monitor the degree of crystallinity of the samples. PXRD data were collected in a PANalytical Empyrean (Malvern PANalytical Ltd., Malvern, UK) diffractometer in reflection mode with copper radiation (Cu K α , $\lambda = 1.5406 \text{ \AA}$) and a secondary monochromator. The tube voltage and amperage were 40 kV and 40 mA, respectively. Each sample was scanned with 2θ between 5° and 40° with a step increment of 0.026° 2θ /step and 113 s per step on a flat stage that was spinning at 4 rpm. The diffraction data was processed using the X'Pert HighScore PlusR software v2.2a (PANalytical BV).

2.5.2. Thermal analysis

Thermal analysis was performed using a Thermal Advantage differential scanning calorimeter (DSC) (Netzsch DSC214 Polyma machine equipped with a refrigerated cooling accessory) that was calibrated for temperature and cell constants using indium and sapphire. Samples (3–5 mg) were weighed, and crimped in non-hermetic aluminium pans (30 μ l). The samples were equilibrated at 30 °C and then scanned at a heating rate of 10 °C/min up to 250 °C under a continuously purged dry nitrogen atmosphere (with a flow rate of 50 ml/min). The data were collected in triplicate for each sample and were analyzed using TA Instruments Universal Analysis 2000 V4.3 A software.

2.5.3. Scanning electron microscopy (SEM)

The SU70 Hitachi (Hitachi, Japan) SEM instruments were used to take images of the generated polymorphs and compare them with the starting material (DOXY.H₂O form I) produced. Each sample was carefully placed on a carbon tape previously placed on top of a SEM 15 mm stub. The samples were then coated with a layer of gold using an Emitech K550 (Emitech, UK) device operating at 20 mA for 60 s. After that, the coated samples were tested with an average working distance of 10 mm, an acceleration voltage of 10 kV, and a 30 μ m aperture. To ensure that the samples were uniform, at least ten pictures were taken.

2.5.4. Fourier transform infrared spectroscopy (FTIR)

In addition, Infrared (IR) spectra of the dry samples of raw material (DOXY.H₂O form I) and generated polymorphs using the UE-SAR process were collected using a PerkinElmer, spectrum 100 spectrometer fitted with universal ATR accessory (single reflection and diamond/zinc selenide material) and lithium tantalate detector. In total, an average accumulation of 256 scans was collected per spectrum over the wave number range from 400 to 4000 cm^{-1} at a resolution of 4 cm^{-1} .

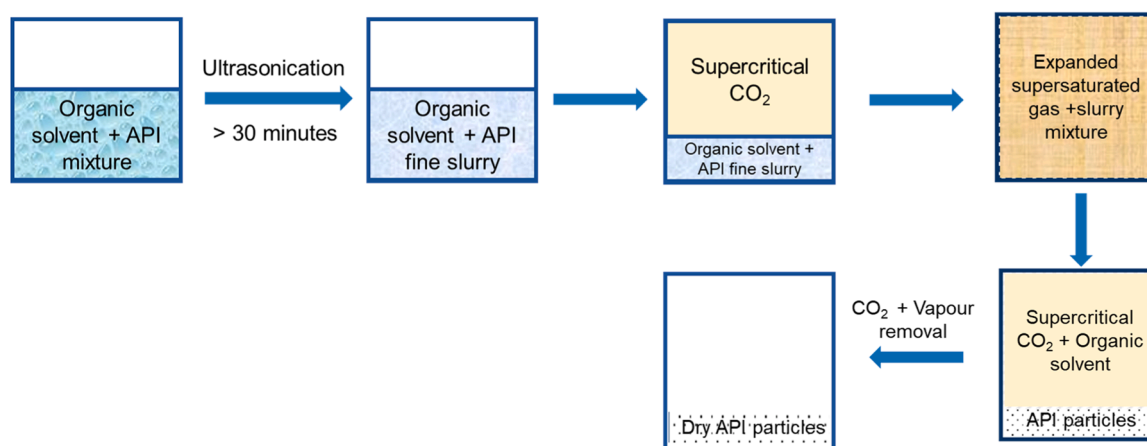


Fig. 4. Process flow diagram of the ultrasonication-enhanced supercritical antisolvent recrystallization (UE-SAR) method for the generation of doxycycline monohydrate (DOXY.H₂O) polymorphs.

Table 3

Summary of the polymorphic form outcome of DOXY-H₂O from the Design of experiments (DoE) study for the supercritical antisolvent recrystallization (SAR) process.

| Sample Reference | Pressure (bar) | Temperature (°C) | Residence time (h) | Polymorphic form |
|------------------|----------------|------------------|--------------------|------------------|
| DoE point 1 | 90 | 25 | 1 | I + II |
| DoE point 2 | 90 | 60 | 1 | I + II |
| DoE point 3 | 200 | 60 | 1 | I + II |
| DoE point 4 | 200 | 25 | 1 | I |
| DoE point 5 | 90 | 25 | 8 | I + II |
| DoE point 6 | 90 | 60 | 8 | I + II |
| DoE point 7 | 200 | 60 | 8 | I |
| DoE point 8 | 200 | 25 | 8 | I + II |
| DoE point 9 | 150 | 40 | 4 | I + II |
| DoE point 9 R* | 150 | 40 | 4 | I + II |

*For DoE point 9 R, agitation speed increased to 1200 rpm, API to ethanol mass ratio increased to 1:50, CO₂ flushing rate thrice.

3. Results and discussion

This paper addresses novel polymorph generation of doxycycline using a conventional supercritical antisolvent recrystallization (SAR) process and a modified SAR process by DoE. As mentioned by Chang et al., increasing pressure of CO₂ also increases miscibility/solubility of the organic solvent in the CO₂, and at higher pressure (denser scCO₂) increases the proportion of organic solvent dissolved in scCO₂ [14,20]. Before conducting this DoE, preliminary experiments were performed at subcritical conditions of compressed CO₂ (pressure of 90 bar, 25 °C, and residence time of 1 h) to ensure that precipitation at these points, the least likely to induce crystallization, would occur. The pressure limits were set in order to maintain affordable compression expenses. The minimum pressure value selected was 90 bar to ensure that CO₂ would

remain in a supercritical state, while 200 bar was selected as the maximum pressure value due to the pressure rating of the equipment. The minimum temperature setting employed was 25 °C to incorporate the effect of high-pressure compressed CO₂ at subcritical temperatures, while the maximum temperature setting was selected to 60 °C based on the maximum value permitted for the experimental setup. Finally, the residence time of crystallization was selected as a process parameter in the DoE, as it is known to influence the rate of polymorphic transformation [21] but has not been investigated for its impact on novel polymorph formation using SAR methods. The residence time of crystallization limits was evaluated at both high and low levels to provide a significant duration for the polymorphic phase transformation to be completed. For rapid mixing, during the SAR processing the contents of the high-pressure vessel were subjected to continuous stirring to ensure precipitation would occur. The range of temperature and residence time of crystallization were selected based on preliminary experiments investigating the ability of the process to produce a sufficiently dried powdered product covering a broader (high-pressure subcritical and supercritical region) working space. All experiments of DoE shown in Table 2 were carried out following the same experimental procedure at operating conditions (high and low levels of each factor). The work presented herein investigates the influence of critical processing parameters as pressure, temperature, and stirring rate using the SAR and UE-SAR methods to assess the outcome of DOXY-H₂O polymorph formation.

3.1. Effect of the SAR process on DOXY-H₂O polymorph generation in DoE based study

Supercritical antisolvent recrystallization (SAR) processing, based on supercritical CO₂, was first explored to obtain new forms of DOXY-H₂O crystals. A DoE approach was taken to investigate the effect of three process parameters, pressure, temperature, and residence time of

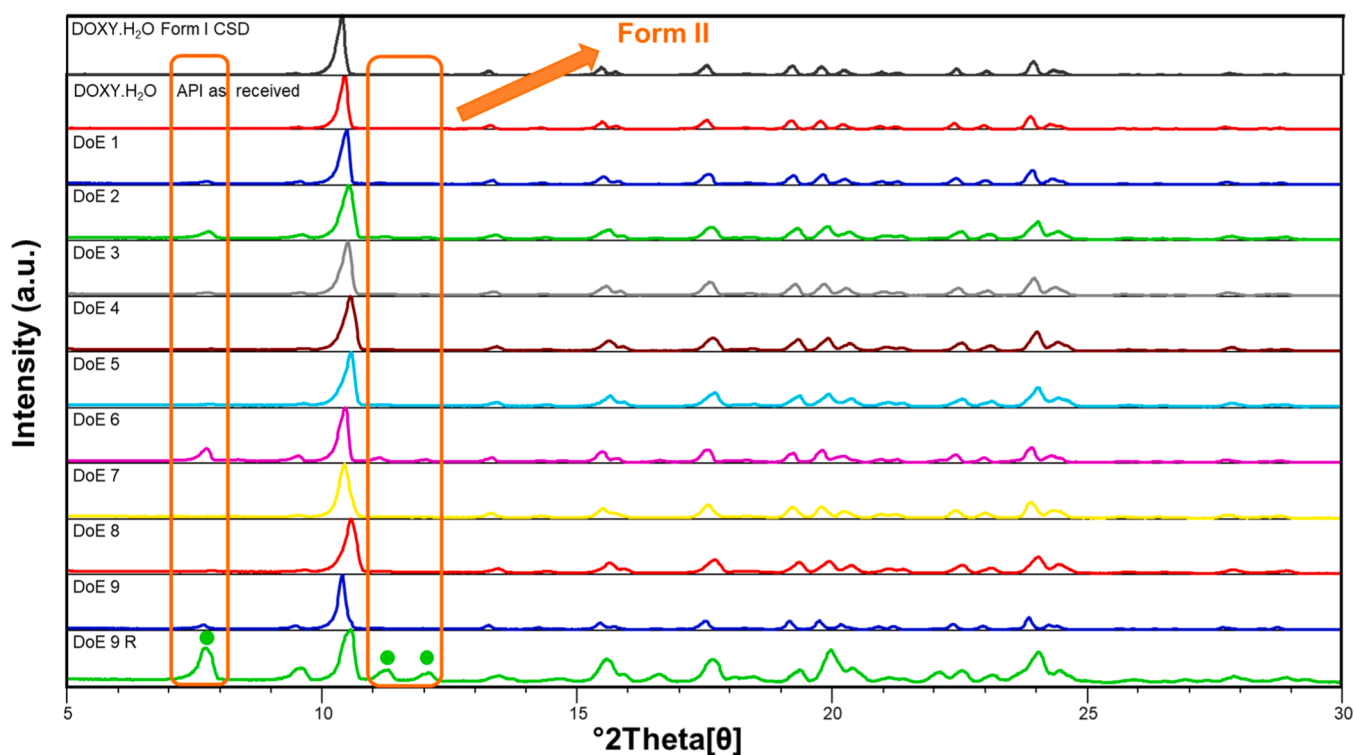


Fig. 5. Powder X-ray diffraction (PXRD) patterns of the theoretical DOXY-H₂O form I from the Cambridge Structural Database (CSD), DOXY-H₂O as received, and DoE samples produced by the supercritical antisolvent recrystallization (SAR) process. Experimental conditions as described in Table 1 (DoE points 1 – 9, and 9 R). Orange rectangular boxes and green rectangular markers (DoE point 9 R) indicate the characteristic peaks of the new DOXY-H₂O form II at 7.71°, 9.52°, 11.05° and 12.02° 2θ.

recrystallization, on the solid-state outcome of the DOXY·H₂O crystals, produced by the SAR process.

Table 3 summarized the DoE study along with operating conditions and corresponding polymorphic form determined by PXRD and highlights the resulting polymorphic outcome of the DOXY·H₂O crystals produced at each set of conditions, as also schematically mentioned in Fig. S.1 diagram.

The PXRD analysis of the SAR processed samples was carried out to evaluate the formation of a new crystalline phase. The resulting diffractograms were compared with those obtained for the unprocessed as-received DOXY·H₂O and the reference spectra from the Cambridge Structural Database (CSD), where the presence of new diffraction peaks suggests a new crystalline phase. The solid-state form and polymorphic purity of the DOXY·H₂O samples were also checked by comparing the patterns from each sample to the reported DOXY·H₂O form I by Santos et al. [22].

The DOXY·H₂O form I presents characteristic peaks at 10.45°, 13.32°, 17.64°, and 19.2° 2 θ , while the DOXY·H₂O form II presents characteristic peaks at 7.71°, 9.52°, 11.05°, and 12.02° 2 θ . In the PXRD patterns of DoE runs (except DoE runs 4 and 7) presented in Fig. 5, it can be observed that the peaks (singlets) at 10.45° and 17.64° 2 θ correspond to the DOXY·H₂O form I and that the singlets at 7.71°, 9.52°, and 11.05° 2 θ correspond to the DOXY·H₂O form II, while only characteristic peaks of DOXY·H₂O form I are found to be present in that of DoE 4 and 7 samples. It was observed that all the reproducible experiments presented the same polymorph outcome (data are shown here).

In the DoE studies conducted for the SAR process, the DOXY·H₂O form I, or a mixture of both DOXY·H₂O forms I and II, were more predominant at all tested conditions. Nonetheless, for the DoE point 9 R run, the peak intensities at 2 θ = 7.71°, 9.52°, 11.05°, and 12.02° increase significantly while the peak related to DOXY·H₂O form I decreases simultaneously. In the DoE 9 R run which was carried out with a higher solvent mass (increased from 1:10–1:50) and increased stirring at 1200 rpm (Table 3), there was a predominance of the DOXY·H₂O form II at 40 °C independently of the residence time of recrystallization and pressure used. Taking into account the experiments conducted for the SAR process, the influence of the processing variables (pressure, temperature, and residence time) was observed to have a lesser effect than the mixing and amount of solvent used. However, after incorporating these changes, PXRD pure DOXY·H₂O form II was unable to be obtained from the SAR process. The outcome of the polymorphic purity is challenging to control, as it was experimentally observed in the recrystallization of DOXY·H₂O by the SAR process.

3.2. Effect of the UE-SAR process on solid-state control of DOXY·H₂O

Supercritical CO₂ antisolvent crystallization typically promotes the formation of metastable polymorphic forms of pharmaceutical drugs. Our rationale is that using this technological approach in combination with the use of ultrasounds can potentially provide further control over the final polymorphic form obtained. Ultrasonication would decrease particle size, and the suspension would look much ‘thinner’, so easier afterwards for all doxy particles (being much smaller) to reconvert into a different polymorphic form with the combined action of scCO₂ and solvent. Ultrasonic waves, when applied to liquids, exhibit a cyclic succession of expansion and compression phases. The expansion cycles pull the molecules apart while the compression cycles apply a positive pressure, pushing the molecules together. In addition, ultrasound waves cause cavitation, which amplifies mass transfer. Cavitation bubbles form in the phase that experiences the bust reduction of pressure caused by ultrasonic waves. The creation, expansion, and eventual collapse of microbubbles release a significant amount of energy. A confined hot spot with high pressure and temperature is created when a bubble bursts, producing strong shock waves. Particles are also broken down by the implosion of vacuum bubbles. Consequently, the solvent and solute particle intimate mixing is improved [11,23–25]. Applying ultrasounds

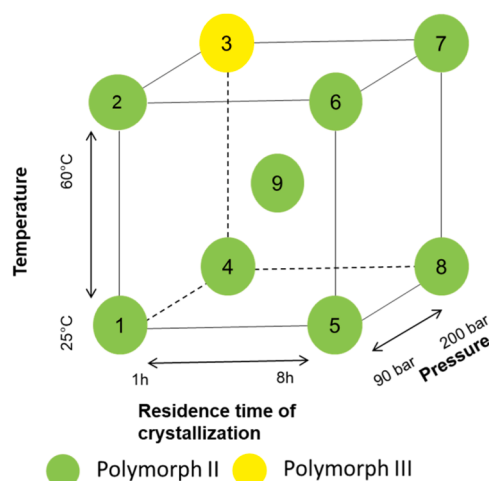


Fig. 6. Schematic outcome of Design of experiments (DoE) study, as described in Table 2 (DoE points 1–9) to assess the impact of pressure, temperature, and residence time for crystallization as process variables on the polymorphic outcome of DOXY·H₂O crystals produced by the ultrasonication-enhanced supercritical antisolvent recrystallization (UE-SAR) process. Green circles indicate the DOXY·H₂O polymorph II, while both colours indicate mixtures of polymorphs I + II, and yellow circles indicate the DOXY·H₂O polymorph III.

in the precipitation chamber has been explored in the literature to enhance the intimate mixing between solute and antisolvent to assist the PXRD pure polymorph generation [26]. The supercritical antisolvent precipitation with enhanced mass transfer (SAS-EM) method (a different supercritical antisolvent method than SAR, where the former uses a nozzle to atomize the drug solution into the supercritical CO₂ phase) was utilized by Jia et al. [27] to regulate the curcumin particle’s morphology and particle size distribution. Those authors found that the speed at which the liquid and scCO₂ mix is accelerated by the ultrasounds [27]. By adjusting the ultrasound power, the various morphologies - such as needle-like, rod-like, irregular lumpy, and nanospherical particles - were produced [5].

Therefore, the SAR process is further modified and refined by the addition of a sonication step prior to the SAR processing. The conditions for the ultrasonication parameters were optimized by preliminary screening experiments and selected based on the visual observation of the homogeneity of the generated fine suspension. Thereafter, a similar DoE-based approach was performed to understand the effect of the ultrasonication-enhanced SAR process on the polymorphic outcome of DOXY·H₂O, as presented in Fig. 6. An additional investigation into the polymorph generation through slow evaporation from the fine suspension after ultrasonication (without SAR processing) of the DOXY·H₂O was also undertaken, allowing the precipitated DOXY·H₂O to remain immersed in the media for a prolonged period.

Fig. 6 and Table S.1 illustrate the PXRD patterns of DOXY·H₂O samples obtained from the UE-SAR process, using ethanol as solvent. The effect of the ultrasonication-enhanced SAR process on the polymorphism of DOXY·H₂O using similar DoE was studied. More than 30 minutes of probe-sonication were applied in each experimental run before the SAR process, as described in Section 2.3.

Fig. 7 shows PXRD diffractograms obtained for the DoE runs 1–9, 10 as described in Table S.1. DoE point 10 (ultrasonication followed by slow evaporation) refers to the fine suspension sample, generated after 35 mins of probe sonication process, dried through slow evaporation in temperature controlled fume hood at 25 °C and under atmospheric pressure. The resulting diffractograms from samples obtained from DoE runs using the UE-SAR process were compared to the predicted diffractogram of DOXY·H₂O form I obtained from the CSD and that of unprocessed as-received DOXY·H₂O, where new diffraction peaks suggest a new polymorphic form.

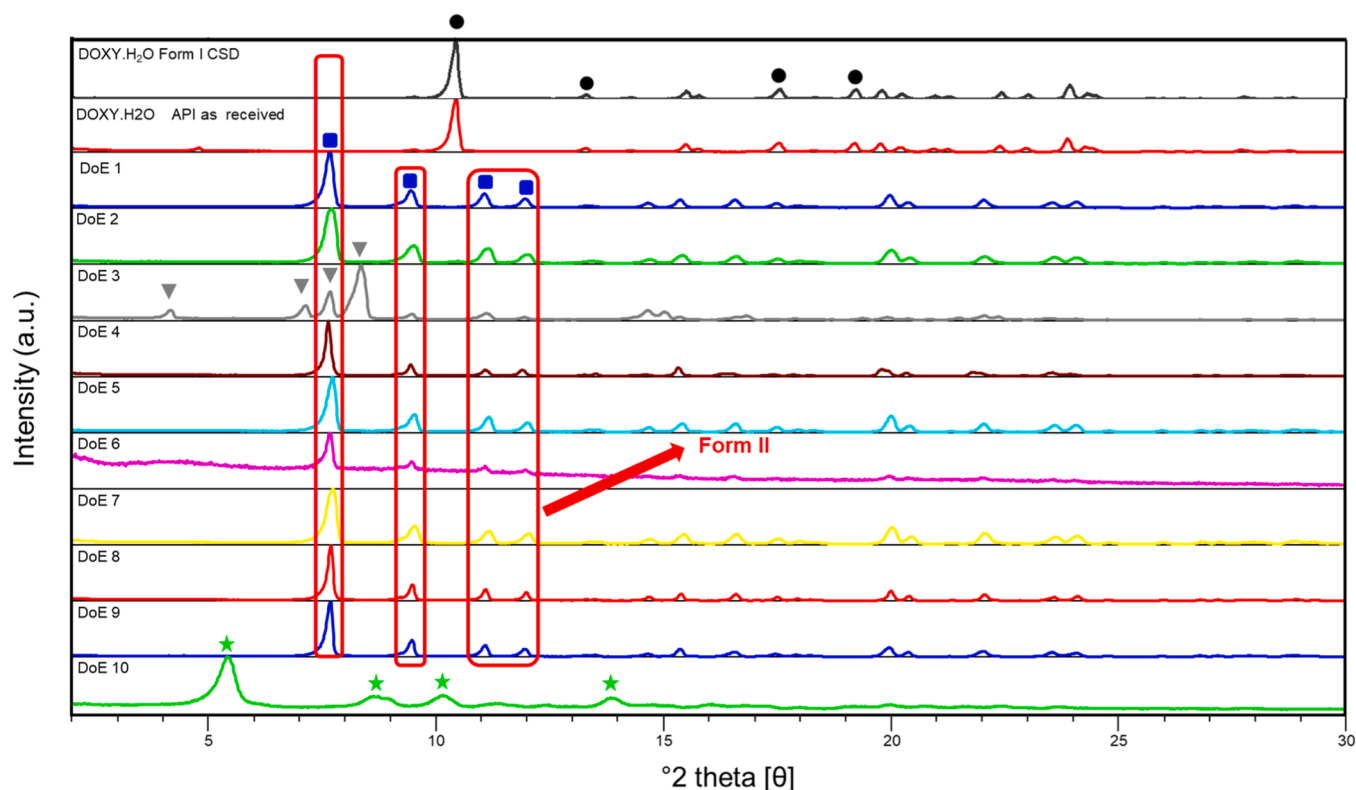


Fig. 7. Powder X-ray diffraction (PXRD) patterns of the theoretical DOXY·H₂O from the Cambridge Structural Database (CSD), DOXY·H₂O as received, and DoE samples produced by the ultrasonication-enhanced supercritical antisolvent recrystallization (UE-SAR) process (DoE points 1–9) and by ultrasonication followed by solvent evaporation (DoE point 10). Experimental conditions as described in Table S 1 (DoE points 1 –10). Solid black circles indicate the characteristic peaks of the DOXY·H₂O form I at 10.45°, 13.32°, 17.64° and 19.2° 2 θ ; solid blue rectangles indicate the characteristic peaks of the DOXY·H₂O form II at 7.71°, 9.52°, 11.05° and 12.02° 2 θ ; inverted grey triangles indicate the characteristic peaks of the DOXY·H₂O form III at 4.12°, 7.12°, 7.85° and 8.32° 2 θ ; solid green stars indicate the characteristic peaks of the DOXY·H₂O form IV at 5.51°, 8.81°, 9°, 10.22° and 13.9° 2 θ .

The earlier study in Section 3.1 using the SAR process revealed that the combination of process variables showed no significant impact on the purity of the final DOXY·H₂O polymorphic form obtained (no sonication was applied during DoE screening studies). However, when using prolonged sonication in the DOXY·H₂O ethanolic suspensions, DOXY·H₂O samples produced from the UE-SAR process correspond to form II (when using processing conditions of DoE points 1, 2, 4–9) or form III (when using processing conditions of DoE point 3). The polymorph produced by the UE-SAR process (at DoE points 1, 2, 4–9) shows characteristic diffraction peaks for a new DOXY·H₂O form II at 2 θ = 7.71°, 9.52°, 11.05°, and 12.02°. In Fig. 7, it is observed that prolonged ultrasonication promotes the formation of novel PXRD-pure polymorphs of DOXY·H₂O, specifically DOXY·H₂O forms II and III. The diffractograms from the different DoE processing runs, except DoE for point 3, are very similar, suggesting that, within the studied conditions, pressure, temperature, and residence time of crystallization have no significant impact on the type of polymorph produced.

For the processing conditions used for the DoE point 3, a novel and stable form of DOXY·H₂O was accidentally discovered through UE-SAR processing. The novel DOXY·H₂O form III was isolated after exposing DOXY·H₂O suspension to scCO₂ at processing conditions of 60 °C, 200 bar and 1 h residence time, having firstly gone through ultrasonication treatment for 35 mins in the UE-SAR process. The PXRD-pure DOXY·H₂O form III exhibits its highest intensity characteristic singlet peak at 4.12° 2 θ , and triplet peaks at 7.12°, 7.85°, and 8.32° 2 θ , as evidenced by the characteristic peaks of the new form not agreeing with previously published data [28,29]

By comparing the two sets of DoEs presented in Sections 3.1 and 3.2, it can be concluded that the incomplete or no transformation for the samples from the SAR studies is no longer observed for the samples

pretreated with ultrasonication, coupled with higher solvent mass and intensive mixing, where the DOXY·H₂O form II was consistently obtained in all cases except for DoE point 3. In these experiments by the UE-SAR process where ultrasonication was applied, the solid-state transformation of DOXY·H₂O was steered toward the formation of the pure DOXY·H₂O form II or III. Ultrasonication promotes in decreasing the doxycycline particle size in suspension, so it facilitates the mediation by scCO₂ of the solid state transformation of doxycycline from form I into forms II or III. This fact indicates that there is a significant impact on the rate of polymorphic transformation by ultrasonication. Therefore, improved polymorphic control is achieved when the UE-SAR is used in the experiments. The novel solid forms are presented here to serve as an example of the usefulness of the UE-SAR process as a tool in polymorph screening.

Moreover, the PXRD pattern of the air dried slow evaporated sample (DoE point 10 in Table S 1) reveals another distinct diffraction pattern with characteristic singlet peaks at 5.51°, 8.81°, 9°, 10.22°, and 13.9° 2 θ . This potentially indicates formation of another novel polymorph of DOXY·H₂O (mentioned in this manuscript as form IV) from ultrasonication-assisted slow evaporation process.

3.3. Solid state characterization of generated polymorphs

The novel polymorphs of DOXY·H₂O reproducibly obtained from the UE-SAR studies were isolated and analyzed by PXRD, DSC, FTIR, Raman, SEM, TGA, and Karl-Fischer titration to identify and characterize their physical, chemical, and crystalline properties. The results obtained from the diffraction, calorimetric, spectroscopic, and microscopic data strongly indicate the formation of multiple novel DOXY·H₂O forms. Still, for unequivocal determination of the polymorphs stoichiometry, allied

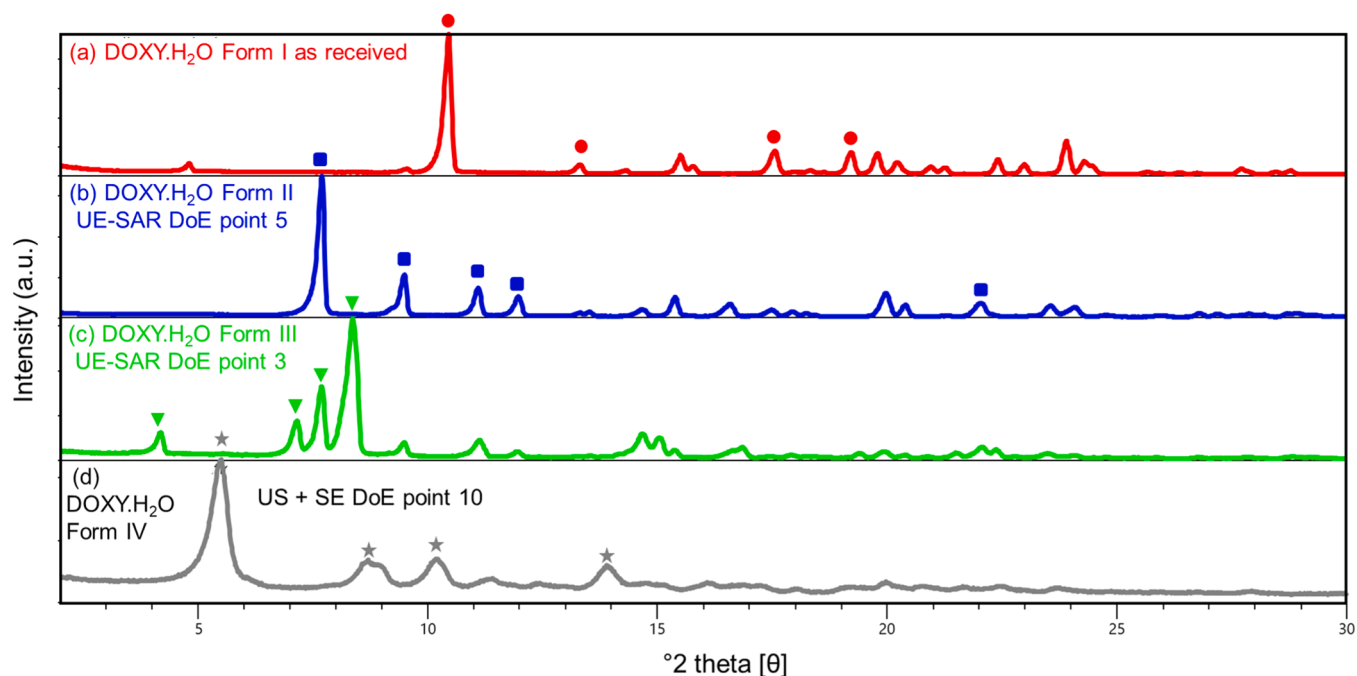


Fig. 8. Powder X-ray diffraction (PXRD) patterns of as-received DOXY·H₂O and of polymorphs of DOXY·H₂O using the ultrasonication-enhanced supercritical antisolvent recrystallization (UE-SAR) process (DOXY·H₂O Forms II and III), and using ultrasonication followed by slow evaporation (DOXY·H₂O Form IV): (a) DOXY·H₂O form I as received, (b) DOXY·H₂O form II (UE-SAR DoE point 5), (c) DOXY·H₂O form III (UE-SAR DoE point 3) and (d) DOXY·H₂O form IV (US + SE DoE point 10). US: Ultrasonication, SE: Slow evaporation. Solid red circles indicate the characteristic peaks of the DOXY·H₂O form I at 10.45°, 13.32°, 17.64° and 19.2° 2θ, solid blue rectangles indicate the characteristic peaks of the DOXY·H₂O form II at 7.71°, 9.52°, 11.05° and 12.02° 2θ, inverted green triangles indicate the characteristic peaks of the DOXY·H₂O form III at 4.12°, 7.12°, 7.85° and 8.32° 2θ, solid grey stars indicate the characteristic peaks of the DOXY·H₂O form IV at 5.51°, 8.81°, 9°, 10.22° and 13.9° 2θ.

with complete structural evaluation, advanced crystallographic analysis such as solid-state NMR-crystallography (ss-NMR) was applied for validation studies specifically for the new DOXY·H₂O form II [30].

3.3.1. Powder X-ray diffraction (PXRD)

PXRD patterns of DOXY·H₂O samples from both as-received and recrystallized forms are shown in Fig. 8. Diffraction peaks of the as-received DOXY·H₂O form I observed from the PXRD analysis were

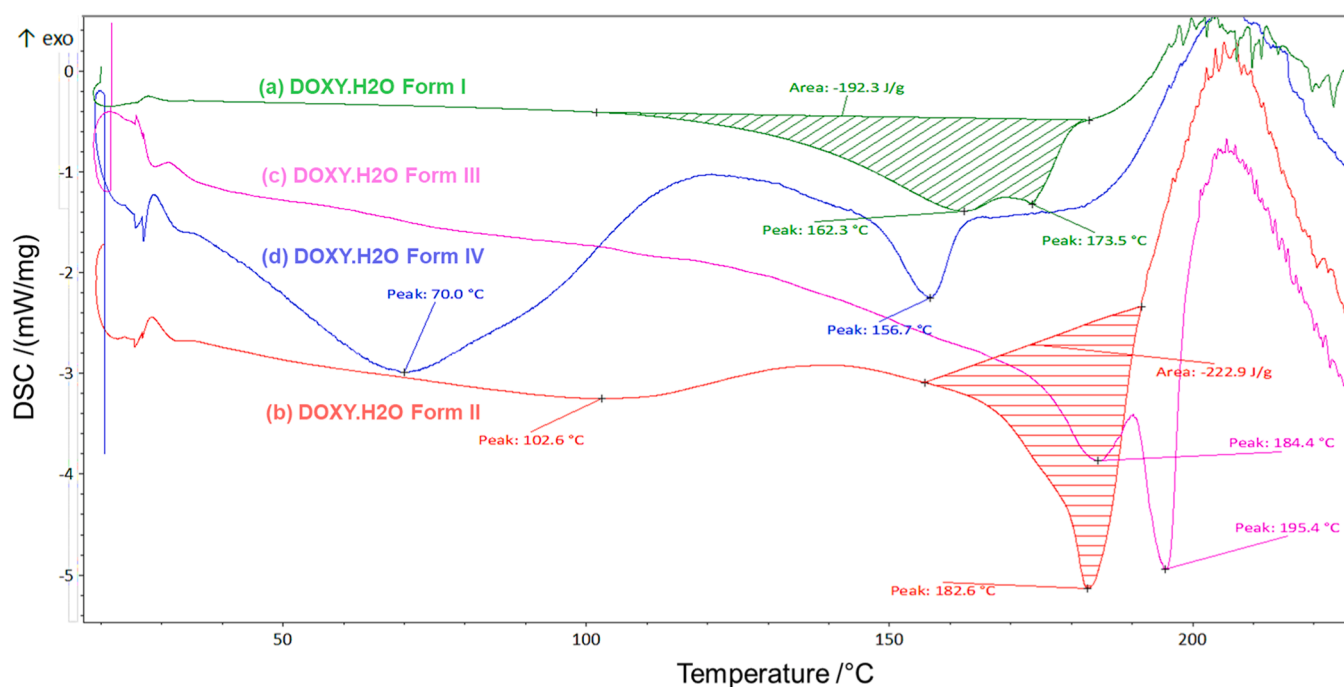


Fig. 9. Differential scanning calorimetry (DSC) analysis of the generated DOXY·H₂O polymorphs using the ultrasonication-enhanced supercritical antisolvent recrystallization (UE-SAR) process: (a) DOXY·H₂O form I as received, (b) DOXY·H₂O form II (DoE point 5), (c) DOXY·H₂O form III (DoE point 3), and (d) DOXY·H₂O form IV (DoE point 10). The melting temperatures are presented at the bottom of each melting peak.

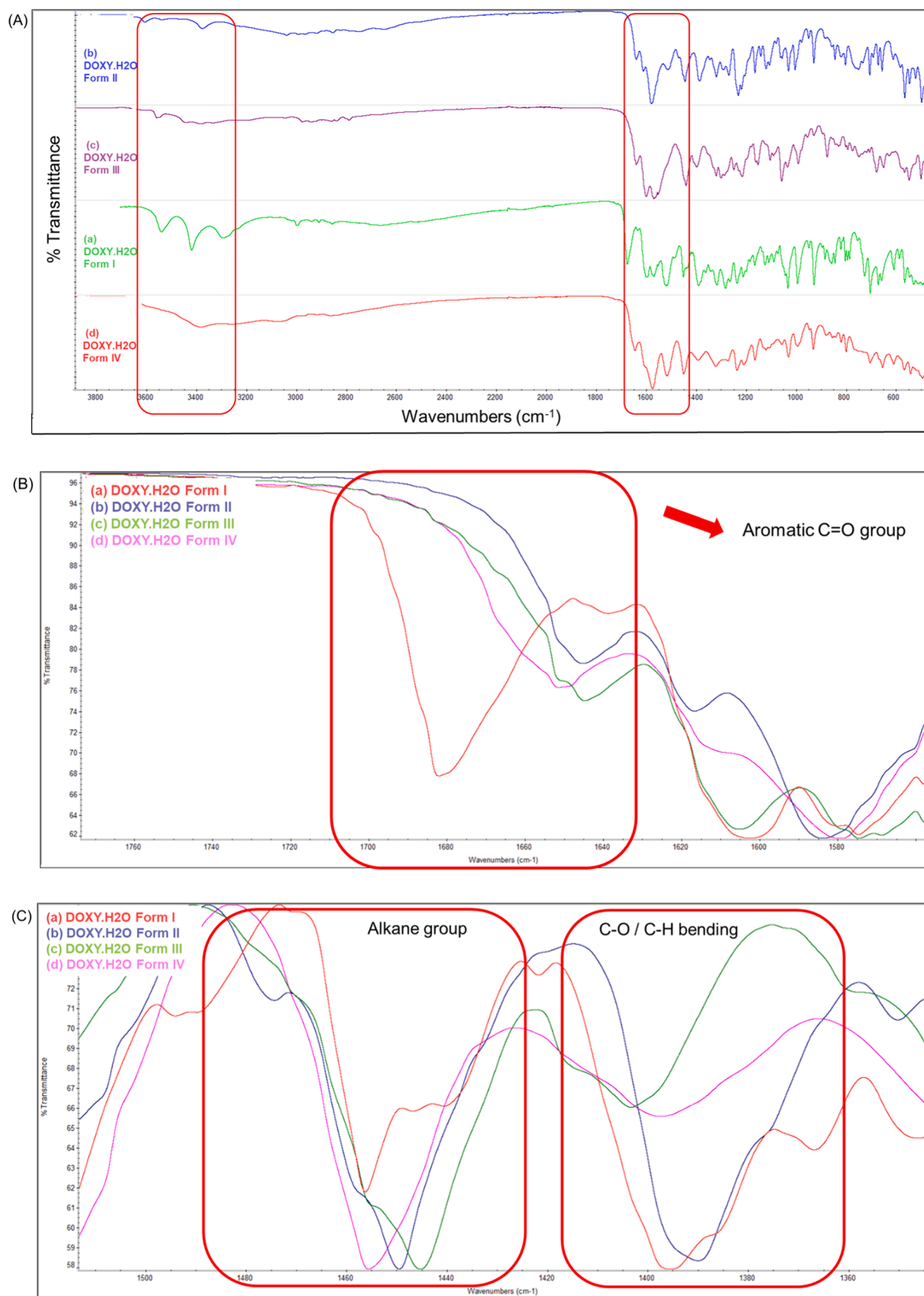


Fig. 10. (A) Fourier-transform Infrared (FTIR) spectra of the generated DOXY·H₂O polymorphs using the ultrasonication-enhanced supercritical antisolvent recrystallization (UE-SAR) process: (a) DOXY·H₂O form I as received, (b) DOXY·H₂O form II (DoE point 5), (c) DOXY·H₂O form III (DoE point 3) and (d) DOXY·H₂O form IV (DoE point 10). The characteristic regions of the polymorphs are highlighted by the red rectangular boxes. (B) Zoomed view of the characteristic region for aromatic C=O group. (C) Zoomed view of the characteristic region for alkane group and C-O / C-H bending of the generated DOXY·H₂O polymorphs.

identical to those observed at diffraction angles of the reference pattern for DOXY·H₂O from the CSD database (previously mentioned), and are also in agreement with the results previously reported by Santos et al. [22]. Furthermore, the produced samples showed sharp peaks, especially within the characteristic region of the PXRD spectra 4–20° 2 θ , which indicates the crystalline structure of the processed DOXY·H₂O samples. The as-received DOXY·H₂O form I presents major characteristic diffraction peaks at 2 θ = 10.45°, 13.32°, 17.64°, and 19.2° (as pointed by the solid circles in Fig. 8(a)). The UE-SAR process DOXY·H₂O form II (UE-SAR DoE point 5) shows major characteristic diffraction peaks at 2 θ = 7.71°, 9.52°, 11.05°, and 12.02° (as pointed by the solid rectangles in Fig. 8(b)), whereas for the DOXY·H₂O form III sample (UE-SAR DoE point 3) the characteristic peaks were at 2 θ = 4.12°, 7.12°, 7.85°, and 8.32° (as pointed by the inverted triangle in Fig. 8(c)). The slowly crystallized DOXY·H₂O sample of UE-SAR DoE point 10 (DOXY·H₂O form IV) show characteristic diffraction peaks at 2 θ = 5.51°, 8.81°, 9°, 10.22°, and 13.9° (as pointed by the stars in Fig. 8(d)).

The new diffraction peaks in the PXRD diffractograms, when compared with those of the as-received DOXY·H₂O form I, suggest the generation of novel polymorphic forms. The differences in 2 θ in the patterns are linked to the variation of molecular arrangements at each orientation. The differences observed in the peak positions of the produced crystals may be due to the impact of the process conditions on the molecular arrangement and crystal packing during precipitation. Since PXRD patterns are "fingerprints" of the crystal structures, indicating the d-spacings between lattice planes formed by the molecules that form the new crystal lattice, this behavior suggest the formation of three novel polymorphs of DOXY·H₂O.

3.3.2. Differential scanning calorimetry (DSC)

Fig. 9 compares the thermograms of recrystallized DOXY·H₂O samples with as-received DOXY·H₂O form I. The DOXY·H₂O form I presents two endothermic peaks at 162.3 °C and 173.5 °C, before the exothermic reaction (decomposition) near 210 °C (Fig. 9(a)). In addition, as showed by DSC analysis, the first endotherm was observed between 90 °C and 165 °C (DSC peak at 162.3 °C) and refers to the loss of bound water in the DOXY·H₂O crystal, followed by melting at 173.5 °C (having enthalpy of fusion, $\Delta_{\text{fus}}H$ = 192.3 J/g), and a final endotherm when thermal decomposition of the sample takes place (DSC peak maximum at 210 °C). The thermogram of the as-received DOXY·H₂O API is similar to the one previously reported by Santos et al. [22] and the melting point (peak maximum at 162.2 °C) of DOXY·H₂O form I has been previously reported by Legendre et al. [29] and others [31]. Regarding the DOXY·H₂O form II (UE-SAR DoE point 5), the thermogram (Fig. 9(b)) shows a first endothermic peak maximum at 102.6 °C, due to water elimination (loss of mass from 60 °C to 145 °C), followed by a second sharp endothermic peak maximum around 182.6 °C ($\Delta_{\text{fus}}H$ = 222.9 J/g) which corresponds to the melting of the sample immediately before its decomposition near 210 °C. In the case of DOXY·H₂O form III (UE-SAR DoE point 3), the thermogram (Fig. 9(c)) shows a first broad endothermic peak maximum at 184.4 °C, which probably due to elimination of bounded water from molecular moiety, possibly corresponding to a solid–solid transition from DOXY·H₂O form II, followed by a second sharp endothermic peak maximum around 195.4 °C ($\Delta_{\text{fus}}H$ = 238.7 J/g) which corresponds to the melting of the sample, which immediately after that decomposition started near 210 °C.

Whereas the thermogram of slowly crystallized DOXY·H₂O form IV (UE-SAR DoE point 10) (Fig. 9(d)) shows a first broad endothermic peak maximum at 70 °C, due to residual ethanol and unbound water elimination (loss of mass from 60 °C to 130 °C), a second endothermic peak maximum at 156.7 °C ($\Delta_{\text{fus}}H$ = 171.4 J/g), which corresponds to the melting of the sample, then baseline up to 200 °C, and after that decomposition started near 210 °C. These results are similar to the data reported by Bratu et al. [32], when studying new solid forms of norfloxacin. Bratu et al. also observed the appearance of an additional endothermic peak in a recrystallized form corresponding to a solid–solid

transition before the melting of the sample [32]. Also, Ali et al. showed that the transition of forms between polymorphs of sulfathiazole observed by DSC thermogram and confirmed by Raman data [33]. The comparison of DSC thermograms shows different enthalpy of fusion values suggesting them to be different forms. The higher numerical value of melting temperature and enthalpy of fusion, $\Delta_{\text{fus}}H$, suggests that form III is the thermodynamically most stable form. The absolute value of enthalpy of fusion along with melting point of DOXY·H₂O followed the order: form IV < form I < form II < form III. This indicates that the stability hierarchy of the DOXY·H₂O polymorphs follow similar pattern. The DSC results presented herein our manuscript indicate the emergence of two new polymorphic forms of DOXY·H₂O upon ultrasonication-assisted recrystallization with supercritical CO₂, which seems to be thermodynamically more stable than form I due to the presence of a higher melting point and subsequently higher $\Delta_{\text{fus}}H$ values, whereas ultrasonication followed by slow evaporation process resulted in another new metastable polymorphic form (DOXY·H₂O form IV). This data strongly supports the PXRD findings.

3.3.3. Fourier transform infrared spectroscopy (FTIR)

The FTIR spectra obtained for each generated DOXY·H₂O form are shown in Fig. 10. The infrared spectrum of as-received DOXY·H₂O form I is similar to the one previously reported [34]. FTIR analysis was used to identify differences in the chemical structure of the generated DOXY·H₂O polymorphs during the applied processes. Since the chemical structure of the generated polymorphic forms are essentially the same, there are no significant differences in their spectra, as previously described by Santos et al. [22]. DOXY·H₂O retained its molecular structure upon processing by the UE-SAR process. The characteristic peaks of DOXY·H₂O are identified at 1663 cm⁻¹, 1612 cm⁻¹, 1576 cm⁻¹, 1554 cm⁻¹, 1458 cm⁻¹, and 1217 cm⁻¹ corresponding to important functional groups in the chemical structure of DOXY·H₂O. DOXY·H₂O showed strong C–H, N–H, and O–H absorption bands between 3500 and 3000 cm⁻¹ and C=O and C=C stretches between 1700 and 1600 cm⁻¹. The crystallized water molecules are represented by bands that appear at around 3550 cm⁻¹ (ν aH₂O) and 1600 cm⁻¹ (δ H₂O) in all four DOXY·H₂O samples. This indicates the presence of the chemical core structure of the doxycycline monohydrate in all obtained polymorphs. The fingerprint region below 1200 cm⁻¹ is almost identical for all DOXY·H₂O forms.

The most notable differences between the DOXY·H₂O polymorphs are observed in the bands arising from carbonyl (ν C=O) and aromatic C–C bonds (ν CCring), which lie in the region from 1700 to 1650 cm⁻¹, 1600–1580 cm⁻¹ (bending vibration, δ H₂O) and 1460–1440 cm⁻¹ (C–H₂ bending), also supported by the results obtained in the Raman spectra further below. The broad bands and shoulders with reduced intensities between 3500 and 3350 cm⁻¹, observed in the case of DOXY·H₂O forms II, III, and IV (wide broad peak), result from the OH stretching of the alcohol, enol, and phenol groups [22,34]. The intense electronic delocalization comprising several atoms next to the amide, ketone, and enol, as well as the abundant amount of hydrogen bonds involving these groups, broadens the ν C=O bands (in all spectra, they are broad and asymmetric). In addition, the decrease in energy of these bands reflects the occurrence of inter- and intramolecular hydrogen bonds. Several spectral features clearly point to the presence of structurally different compounds. For example, the absorption bands assigned to stretching O–H at 3600 cm⁻¹ (possibly non-hydrogen bonded OH groups), 1640–1650 cm⁻¹ (shift and broadening of peaks related to δ C=O and δ C=C) and shift in C–H₂ bending (at 1452 cm⁻¹ DOXY·H₂O form I (as received API), at 1450 cm⁻¹ DOXY·H₂O form II (UE-SAR DoE point 5), at 1445 cm⁻¹ DOXY·H₂O form III (UE-SAR DoE point 3), and 1456 cm⁻¹ DOXY·H₂O form IV (UE-SAR DoE point 10)) are only well resolved in structurally different spectra of the same DOXY·H₂O compound. Therefore, the infrared data suggests that the UE-SAR process, along with the method used in DoE point 10 (ultrasonication followed by solvent evaporation, as referred to in Table 2 and S.1), has

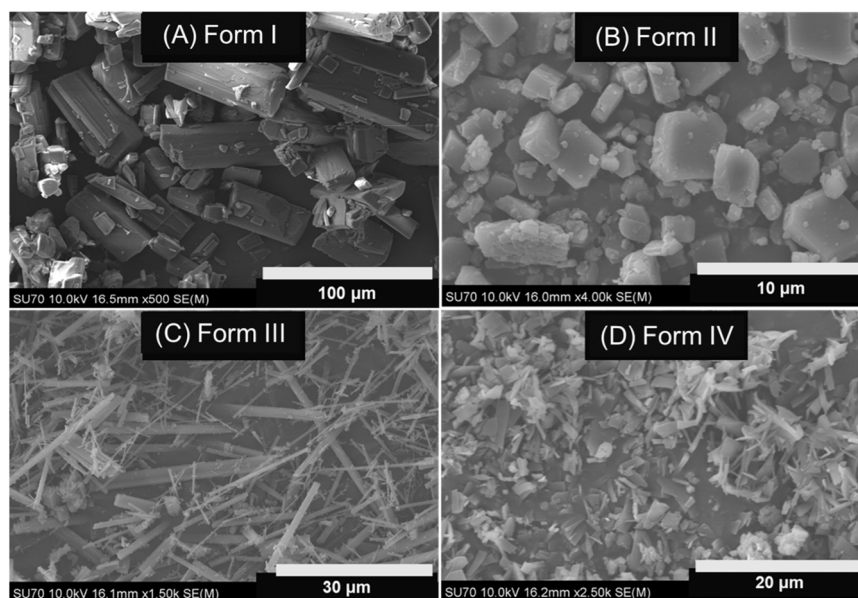


Fig. 11. Scanning electron microscopy (SEM) images of the generated DOXY·H₂O polymorphs using the ultrasonication-enhanced supercritical antisolvent recrystallization (UE-SAR) process: (A) DOXY·H₂O form I as received, (B) DOXY·H₂O form II (DoE point 5), (C) DOXY·H₂O form III (DoE point 3) and (D) DOXY·H₂O form IV (DoE point 10).

generated three distinct new doxycycline forms (DOXY·H₂O forms II, III, and IV) from the as-received DOXY·H₂O form I.

3.3.4. Scanning electron microscopy (SEM)

Fig. 11 shows scanning electron microscopy images of the crystal morphology of the DOXY·H₂O samples: form I (as received API), forms II (DoE point 5) and III (DoE point 3), form IV (DoE point 10) obtained from the UE-SAR process, respectively. A wide variation of crystal habits can be observed for each polymorph of DOXY·H₂O.

The untreated as-received DOXY·H₂O crystals were orthorhombic in shape (Fig. 11 (A)). The SEM image of the DOXY·H₂O form II displays small homogenous rectangular tabular-shaped crystals with a smooth surface (Fig. 11 (B)), whereas the morphology of DOXY·H₂O form III shows a needle-like crystal (Fig. 11 (C)). DOXY·H₂O form IV obtained after ultrasonication followed by slow evaporation at room temperature resulted in elongated thin plate-shaped morphology (Fig. 11 (D)). The varied morphologies obtained for different DOXY·H₂O forms have been linked to the variation of molecular arrangement in the solute lattice or to its interaction with the growing crystal surface. The application of ultrasonication before the SAR process, or before the slow evaporation process, resulted in small micron-sized particles.

4. Conclusions

From the DoE studies using the SAR process, either a mixture of DOXY·H₂O forms I and II, or only the DOXY·H₂O form I, were obtained due to partial or no polymorphic conversion. The application of prolonged ultrasonication and increasing agitation speed, along with solvent-to-solids ratio, promoted the formation of pure and new polymorphs of DOXY·H₂O. The combination of the highest pressure and temperature promoted the formation of DOXY·H₂O form III, whereas the rest of the DoE conditions yielded pure DOXY·H₂O form II in the case of the US-SAR process. Additionally, the slow evaporation process resulted in the generation of an additional new form (DOXY·H₂O form IV). The DOXY·H₂O crystals were characterized by several solid-state techniques (PXRD, SEM, DSC, Raman, FTIR, and Karl Fisher), and all data comply with the formation of new DOXY forms. The newly discovered DOXY·H₂O forms II and III showed a considerably higher thermostability (with a melting point of 182 and 195 °C, respectively). The structures of

DOXY·H₂O forms I and II were further elucidated by ss-NMR from ¹³C and ¹⁵N CP/MAS spectra. These findings point out three directions to follow-up on in future research articles: one regarding formulation development using DOXY·H₂O forms II and III, structure elucidation of forms III and IV using ss-NMR, and further use of the UE-SAR process as a route for the exploration of novel polymorphs of other APIs. Overall, the findings in this work show that it is possible to skip the requirement for an API to fully dissolve in an organic solvent or in scCO₂ to perform solid-state polymorphic transformation.

CRediT authorship contribution statement

Nandi Snehashis: Writing – review & editing, Writing – original draft, Visualization, Software, Methodology, Investigation, Formal analysis, Data curation. **Padrela Luis:** Writing – review & editing, Supervision, Resources, Project administration, Methodology, Investigation, Funding acquisition, Conceptualization. **Nunes Teresa G.:** Writing – review & editing, Validation, Software, Formal analysis, Data curation. **Duarte Andreia:** Investigation, Formal analysis, Data curation. **Rodrigues Miguel Angelo:** Writing – review & editing, Writing – original draft, Supervision, Methodology, Investigation, Funding acquisition, Formal analysis, Conceptualization.

Declaration of Competing Interest

The authors declare that they have no known competing financial interests or personal relationships that could have appeared to influence the work reported in this paper.

Acknowledgements

For financial Support, L.P. and N.S. acknowledge the European Union's Horizon 2020 Research and Innovation Program under the Marie Skłodowska-Curie grant agreement process (grant no. 861278). L. P further acknowledges Research Ireland for supporting the work undertaken at the SSPC Research Centre (Phase II grant no. 12/RC/2775_P2) and the work undertaken as part of the SFI Frontiers for the Future (grant no. 19/FFP/6896). M.A.R. acknowledges Fundação para a Ciência e Tecnologia (FCT), Lisbon (grant no. RECI/QEQ-QIN/0189/

2012). L.P. and M.A.R. thank Prof. Edmundo Gomes de Azevedo for the initial discussions and for the preliminary research activities in this work in his laboratory.

Appendix A. Supporting information

Supplementary data associated with this article can be found in the online version at [doi:10.1016/j.jcou.2025.103082](https://doi.org/10.1016/j.jcou.2025.103082).

Data availability

Data will be made available on request.

References

- [1] I. Pasquali, R. Bettini, F. Giordano, Solid-state chemistry and particle engineering with supercritical fluids in pharmaceuticals, *Eur. J. Pharm. Sci.* 27 (2006) 299–310, <https://doi.org/10.1016/j.ejps.2005.11.007>.
- [2] I.A. Cuadra, A. Cabañas, J.A.R. Cheda, C. Pando, Polymorphism in the co-crystallization of the anticonvulsant drug carbamazepine and saccharin using supercritical CO₂ as an anti-solvent, *J. Supercrit. Fluids* 136 (2018) 60–69, <https://doi.org/10.1016/j.supflu.2018.02.004>.
- [3] J. Tian, S.J. Dalgarno, J.L. Atwood, A new strategy of transforming pharmaceutical crystal forms, *J. Am. Chem. Soc.* 133 (2011) 1399–1404, <https://doi.org/10.1021/ja107617m>.
- [4] S.D. Thakore, A. Sood, A.K. Bansal, Emerging role of primary heterogeneous nucleation in pharmaceutical crystallization, *Drug Dev. Res* 81 (2020) 3–22, <https://doi.org/10.1002/ddr.21622>.
- [5] R. Kumar, A.K. Thakur, G. Kali, K.C. Pitchaiah, R.K. Arya, A. Kulabhi, Particle preparation of pharmaceutical compounds using supercritical antisolvent process: current status and future perspectives, *Drug Deliv. Transl. Res* 13 (2023) 946–965, <https://doi.org/10.1007/s13346-022-01283-7>.
- [6] L. Padrela, J. Zeglinski, K.M. Ryan, Insight into the role of additives in controlling polymorphic outcome: a CO₂ antisolvent crystallization process of carbamazepine, *Cryst. Growth Des.* 17 (2017) 4544–4553, <https://doi.org/10.1021/acs.cgd.7b00163>.
- [7] I. Pasquali, R. Bettini, F. Giordano, Solid-state chemistry and particle engineering with supercritical fluids in pharmaceuticals, *Eur. J. Pharm. Sci.* 27 (2006) 299–310, <https://doi.org/10.1016/j.ejps.2005.11.007>.
- [8] M. Amani, N. Saadati Ardestani, N.Y. Majid, Utilization of supercritical CO₂ gas antisolvent (GAS) for production of Capecitabine nanoparticles as anti-cancer drug: Analysis and optimization of the process conditions, *J. CO₂ Util.* 46 (2021) 101465, <https://doi.org/10.1016/j.jcou.2021.101465>.
- [9] N. Esfandiari, S.A. Sajadian, CO₂ utilization as gas antisolvent for the pharmaceutical micro and nanoparticle production: a review, *Arab. J. Chem.* 15 (2022) 104164, <https://doi.org/10.1016/j.arabjc.2022.104164>.
- [10] F. Rezaee, S.M. Ghoreishi, N. Saadati Ardestani, Precipitation of advanced nanomedicines (curcumin) using supercritical processing: experimental study, design and optimizing operating conditions, *J. Drug Deliv. Sci. Technol.* 99 (2024) 105989, <https://doi.org/10.1016/j.jddst.2024.105989>.
- [11] G. Sodeifian, S.A. Sajadian, R. Derakhsheshpour, CO₂ utilization as a supercritical solvent and supercritical antisolvent in production of sertraline hydrochloride nanoparticles, *J. CO₂ Util.* 55 (2022) 101799, <https://doi.org/10.1016/j.jcou.2021.101799>.
- [12] M.A. Rodrigues, J.M. Tiago, A. Duarte, V. Geraldes, H.A. Matos, E. Gomes Azevedo, Polymorphism in pharmaceutical drugs by supercritical CO₂ processing: clarifying the role of the antisolvent effect and atomization enhancement, *Cryst. Growth Des.* 16 (2016) 6222–6229, <https://doi.org/10.1021/acs.cgd.6b00697>.
- [13] D. Jafari, I. Yarnezhad, S.M. Nowee, S.H.N. Baghban, Gas-antisolvent (GAS) crystallization of aspirin using supercritical carbon dioxide: experimental study and characterization, *Ind. Eng. Chem. Res.* 54 (2015) 3685–3696, <https://doi.org/10.1021/ie5046445>.
- [14] N.S. Ardestani, M. Amani, Production of anthraquinone Violet 3RN nanoparticles via the GAS process: optimization of the process parameters using Box-Behnken design, *Dyes Pigments* 193 (2021) 109471, <https://doi.org/10.1016/j.dyepig.2021.109471>.
- [15] T. Ziegler, C. Winkler, K. Wege, H. Schmechel, Doxycycline – das vergessene Antibiotikum, *Med. Klin.* 95 (2000) 629–631, <https://doi.org/10.1007/PL00002075>.
- [16] M.O. Griffin, E. Fricovsky, G. Ceballos, F. Villarreal, Tetracyclines: a pleiotropic family of compounds with promising therapeutic properties. Review of the literature, *Am. J. Physiol. -Cell Physiol.* 299 (2010) C539–C548, <https://doi.org/10.1152/ajpcell.00047.2010>.
- [17] M.A. Rodrigues, J.M. Tiago, L. Padrela, H.A. Matos, T.G. Nunes, L. Pinheiro, A. J. Almeida, E.G. de Azevedo, New thermoresistant polymorph from CO₂ recrystallization of minocycline hydrochloride, *Pharm. Res* 31 (2014) 3136–3149, <https://doi.org/10.1007/s11095-014-1406-3>.
- [18] R. Injac, V. Djordjevic-Milic, B. Srdjenovic, Thermostability Testing and Degradation Profiles of Doxycycline in Bulk, Tablets, and Capsules by HPLC, *J. Chromatogr. Sci.* 45 (2007) 623–628, <https://doi.org/10.1093/chromsci/45.9.623>.
- [19] A.O. Legendre, L.R.R. Silva, D.M. Silva, I.M.L. Rosa, L.C. Azarias, P.J. de Abreu, M. B. de Araujo, P.P. Neves, C. Torres, F.T. Martins, A.C. Doriguetto, Solid state chemistry of the antibiotic doxycycline: structure of the neutral monohydrate and insights into its poor water solubility, *CrystEngComm* 14 (2012) 2532–2540, <https://doi.org/10.1039/C1ce06181j>.
- [20] C.J. Chang, The solubility of carbon dioxide in organic solvents at elevated pressures, *Fluid Phase Equilib.* 74 (1992) 235–242, [https://doi.org/10.1016/0378-3812\(92\)85064-F](https://doi.org/10.1016/0378-3812(92)85064-F).
- [21] C. Neurohr, A.-L. Revelli, P. Billot, M. Marchivie, S. Lecomte, S. Laugier, S. Massip, P. Subra-Paternault, Naproxen–nicotinamide cocrystals produced by CO₂ antisolvent, *J. Supercrit. Fluids* 83 (2013) 78–85, <https://doi.org/10.1016/j.supflu.2013.07.008>.
- [22] O.M.M. Santos, D.M. Silva, F.T. Martins, A.O. Legendre, L.C. Azarias, I.M.L. Rosa, P.P. Neves, M.B. de Araujo, A.C. Doriguetto, Protonation pattern, tautomerism, conformerism, and physicochemical analysis in new crystal forms of the antibiotic doxycycline, *Cryst. Growth Des.* 14 (2014) 3711–3726, <https://doi.org/10.1021/cg500877z>.
- [23] C. Bartos, Á. Kukovecz, R. Ambrus, G. Farkas, N. Radacs, P. Szabó-Révész, Comparison of static and dynamic sonication as process intensification for particle size reduction using a factorial design, *Chem. Eng. Process.: Process Intensif.* 87 (2015) 26–34, <https://doi.org/10.1016/j.cep.2014.10.015>.
- [24] A. Alshweiat, G. Katona, I. Csóka, R. Ambrus, Design and characterization of loratadine nanosuspension prepared by ultrasonic-assisted precipitation, *Eur. J. Pharm. Sci.* 122 (2018) 94–104, <https://doi.org/10.1016/j.ejps.2018.06.010>.
- [25] S. Zhao, Q. Zhao, C. Yao, G. Chen, Investigation of anti-clogging mechanism of ultrasound-driven oscillating slugs/bubbles and its application on continuous crystallization process, *Chem. Eng. Sci.* 290 (2024) 119898, <https://doi.org/10.1016/j.ces.2024.119898>.
- [26] I. Partheniadis, R.R. Shah, I. Nikolakakis, Application of ultrasonics for nanosizing drugs and drug formulations, *J. Dispers. Sci. Technol.* 43 (2022) 1587–1602, <https://doi.org/10.1080/01932691.2021.1878035>.
- [27] J. Jia, W. Wang, Y. Gao, Y. Zhao, Controlled morphology and size of curcumin using ultrasound in supercritical CO₂ antisolvent, *Ultrason Sonochem.* 27 (2015) 389–394, <https://doi.org/10.1016/j.ultsonch.2015.06.011>.
- [28] W. Song, J. Seta, L. Chen, C. Bergum, Z. Zhou, P. Kanneganti, R.E. Kast, G. W. Auner, M. Shen, D.C. Markel, W. Ren, X. Yu, Doxycycline-loaded coaxial nanofiber coating of titanium implants enhances osseointegration and inhibits *Staphylococcus aureus* infection, *Biomed. Mater.* 12 (2017) 045008, <https://doi.org/10.1088/1748-605X/aa6a26>.
- [29] A.O. Legendre, L.R.R. Silva, D.M. Silva, I.M.L. Rosa, L.C. Azarias, P.J. de Abreu, M. B. de Araujo, P.P. Neves, C. Torres, F.T. Martins, A.C. Doriguetto, Solid state chemistry of the antibiotic doxycycline: structure of the neutral monohydrate and insights into its poor water solubility, *CrystEngComm* 14 (2012) 2532–2540, <https://doi.org/10.1039/C1ce06181j>.
- [30] J.L. Dias, E.A. Rebelatto, D. Hotza, A.J. Bortoluzzi, M. Lanza, S.R.S. Ferreira, Production of quercetin-nicotinamide cocrystals by gas antisolvent (GAS) process, *J. Supercrit. Fluids* 188 (2022) 105670, <https://doi.org/10.1016/j.supflu.2022.105670>.
- [31] J. de Freitas, A.P.G. Ferreira, É.T.G. Cavalheiro, Investigating the thermal behavior of doxycycline and meclizine, *J. Therm. Anal. Calor.* 147 (2022) 13413–13423, <https://doi.org/10.1007/s10973-022-11596-x>.
- [32] I. Bratu, G. Borodi, I. Kacsó, Z. Moldovan, C. Filip, F. Dragan, M. Vasilescu, S. Simon, New solid form of norfloxacin: structural studies, *Spectroscopy* 25 (2011) 53–62, <https://doi.org/10.1155/2011/462913>.
- [33] H.R.H. Ali, H.G.M. Edwards, I.J. Scowen, Insight into thermally induced solid-state polymorphic transformation of sulfathiazole using simultaneous *in situ* Raman spectroscopy and differential scanning calorimetry, *J. Raman Spectrosc.* 40 (2009) 887–892, <https://doi.org/10.1002/jrs.2189>.
- [34] D. Tchoň, A. Makal, M. Gutmann, K. Woźniak, Doxycycline hydrate and doxycycline hydrochloride dihydrate – crystal structure and charge density analysis, *Z. Krist. Cryst. Mater.* 233 (2018) 649–661, <https://doi.org/10.1515/zkri-2018-2058>.